0031-3998/04/5604-0553
PEDIATRIC RESEARCH
Vol. 56, No. 4, 2004
Printed in U.S.A.

Respiratory Adaptations to Lung Morphological Defects in Adult Mice Lacking *Hoxa5* Gene Function

RICHARD KINKEAD, MICHELLE LEBLANC, ROUMIANA GULEMETOVA, MÉLANIE LALANCETTE-HÉBERT, MARGOT LEMIEUX, ISABEL MANDEVILLE, AND LUCIE JEANNOTTE

Département de Pédiatrie [R.K., R.G.], Centre Hospitalier Universitaire de Québec, Centre de recherche de l'Hôpital St-François d'Assise, Québec, Canada, G1L 3L5, Centre de recherche en cancérologie de l'Université Laval [M.LeB., M.L.-H., M.Lem., I.M., L.J.], Centre Hospitalier Universitaire de Québec, L'Hôtel-Dieu de Québec, Québec, Canada, G1R 2J6

ABSTRACT

The *Hoxa5* mutation is associated with a high perinatal mortality rate caused by a severe obstruction of the laryngotracheal airways, pulmonary dysmorphogenesis, and a decreased production of surfactant proteins. Surviving *Hoxa5*$^{-/-}$ mutant mice also display lung anomalies with deficient alveolar septation and areas of collapsed tissue, thus demonstrating the importance of *Hoxa5* throughout lung development and maturation. Here, we address the functional consequences of the *Hoxa5* mutation on respiration and chemoreflexes by comparing the breathing pattern of *Hoxa5*$^{-/-}$ mice to that of wild-type animals under resting conditions and during exposure to moderate ventilatory stimuli such as hypoxia and hypercapnia. Resting *Hoxa5*$^{-/-}$ mice present a higher breathing frequency and overall minute ventilation that likely compensate for their reduced lung alveolar surface available for gas exchange and their increased upper airway resistance. When exposed to ventilatory stimuli, *Hoxa5*$^{-/-}$ mice maintain the higher minute ventilation by adapting the tidal volume and/or the breathing frequency. The minute ventilation increase seen during hypoxia was similar for both groups of mice; however, the dynamics of the frequency response was genotype-dependent. The hypercapnic ventilatory response did not differ between genotypes. These findings reveal the strategies allowing survival of *Hoxa5*$^{-/-}$ mice facing morphologic anomalies leading to a significant deficit in gas exchange capacity. **(*Pediatr Res* 56: 553–562, 2004)**

Abbreviations

F_{ICO_2}, fractional concentration of carbon dioxide in the inspired gas
F_{IO_2}, fractional concentration of oxygen in the inspired gas
Tb, body temperature
T_E, expiratory duration
T_I, inspiratory duration
$\dot{V}CO_2$, metabolic production rate of carbon dioxide
V_D/V_T, physiologic dead space to tidal volume ratio
V_T/T_I, inspiratory flow

Hox genes encode a highly conserved family of transcription factors that play a crucial role in embryonic pattern formation in a broad spectrum of species. In mammals, 39 *Hox* genes are arrayed in four clusters (*HoxA* to *D*), each located on a different chromosome. Based on sequence similarity and relative position within the complex, the *Hox* genes have been subdivided into paralogous groups 1–13. The group assignment also reflects both the organization of the *Hox* genes along the complexes and their spatio-temporally coordinated expression along the anteroposterior axis of the embryo. The smaller the number of the paralogous group is, the earlier and the more anteriorly are the genes expressed along the body axis (1).

Genetic analyses of *Hox* mutant mice have revealed a wide variety of structures that require *Hox* gene function for their proper development. *Hox* genes are involved in the neuronal patterning of the hindbrain, the regional specification of the skeleton, and the formation of several organs (2–7). Although the function of *Hox* genes during embryonic development is well established, their postnatal role remains more obscure. Many *Hox* genes present a specific expression profile in adult tissues. Furthermore, characterization of *Hox* mutants has revealed unforeseen postnatal phenotypes, indicating the large range of action of *Hox* genes throughout life (8–10). In the mouse, *Hox* genes, predominantly from paralogous groups 2 to

Received January 21, 2004; accepted April 8, 2004.
Correspondence: Richard Kinkead, Ph.D., Centre de recherche de l'Hôpital St-François d'Assise, 10 rue de l'Espinay (D0–711), Québec, QC, Canada G1L 3L5; e-mail: Richard.Kinkead@crsfa.ulaval.ca
Supported by grants from the Canadian Institutes of Health Research (L.J.) and the Fondation de la Recherche sur les Maladies Infantiles (R.K.). L.J. holds a Chercheur National Award from the Fonds de la Recherche en Santé du Québec, and R.K. is the chairholder of the Canada Research Chair in respiratory neurobiology.

DOI: 10.1203/01.PDR.0000139427.26083.3D

6, are expressed in a distinct spatio-temporal fashion during lung ontogeny, thereby supporting their involvement in regional lung specification and function (11–14). Loss-of-function mutations for several lung-expressed *Hox* genes have been generated, but the consequences on the respiratory tract development and function have been examined for only a handful of these *Hox* mutants. For example, mutation of the *Hoxa1* gene results in perinatal death caused by anoxia, a problem due to alterations of hindbrain segmentation and patterning resulting in the mis-specification of neurons involved in respiratory rhythm generation (15–17).

Hoxa3 and *Hoxa5* genes are also involved in the respiratory system morphogenesis, both being essential for the formation of the larynx (18–20). In addition, *Hoxa5* mutant mice exhibit a disorganized trachea with a complete occlusion of the lumen in the most severely affected animals, and lung dysmorphogenesis accompanied by a reduced branching of the bronchial tree and a decreased production of surfactant proteins. Collectively, these defects underlie the high rate of perinatal lethality of *Hoxa5*$^{-/-}$ newborns (20). *Hoxa5* is also strongly expressed in adult lung from human and mouse, suggesting that it is involved in the maintenance and/or the function of the organ (21,22). This is further supported by the altered expression of the *HOXA5* gene observed in some pulmonary pathologic conditions in humans: whereas *HOXA5* is overexpressed in patients suffering from primary pulmonary hypertension, its expression is decreased in emphysematous lungs (22). The latter data correlate with our observations of regions with deficient alveolar septation, airspace enlargement and areas of collapsed tissue in the lungs of surviving *Hoxa5*$^{-/-}$ animals (2). Because of its severe lung phenotype, the *Hoxa5* mutation appears to be less subject to compensation by other *Hox* genes, indicating that the *Hoxa5* gene may be important for the structural and functional integrity of postnatal lung.

The airspace enlargement associated with the murine *Hoxa5* loss of function decreases the lung surface area available for gas exchange. Despite some transient growth problems in the first weeks after birth (23), surviving *Hoxa5*$^{-/-}$ mice appear to develop normally, suggesting that these animals have adapted their ventilatory activity to meet this anatomical limitation. Thus, the first objective of the present study was to address how the respiratory control system adapts and compensates for severe deficits in gas exchange capacity by comparing the breathing pattern of *Hoxa5*$^{-/-}$ mice to that of wild-type animals under resting conditions. Because these respiratory defects likely compromise the ability to maintain gas exchange homeostasis, we also tested the hypothesis that *Hoxa5*$^{-/-}$ mice counteract for these limitations by increasing their ability to detect and respond to fluctuations in arterial O_2 and CO_2 levels. To this aim, we compared ventilatory activity of wild-type and mutant mice during exposure to moderate ventilatory stimuli such as hypoxia ($F_{IO_2} = 0.12$) and hypercapnia ($F_{ICO_2} = 0.05$).

MATERIALS AND METHODS

Mouse strain, genotyping, and husbandry. The *Hoxa5* mutant mouse line used in the present study was maintained in a mixed MF1-129/SvEv-C57BL/6 genetic background. Production of the mutant mouse line and genotyping of the mice by Southern analysis have been previously reported (21,24).

The functional consequences of abnormal lung development associated with the *Hoxa5* gene mutation were assessed by comparing the respiratory function and chemoreflexes of wild-type and *Hoxa5*$^{-/-}$ mice. Measurements of ventilatory activity were performed on 31 adult mice, including 14 wild-type mice aged 53 ± 2 d and 17 *Hoxa5*$^{-/-}$ mice aged 55 ± 1 d (Table 1). Animals were supplied with food and water *ad libitum* and they were maintained in standard laboratory conditions (20°C; 12 h/12 h light/dark cycle with light onset at 0600 h). Body and wet lung weights were obtained by direct measurements.

Ventilatory measurements were performed under "resting" conditions (normoxia, $F_{IO_2} = 0.21$; normocapnia, $F_{ICO_2} = 0.003$) followed by exposure to either one of two ventilatory stimuli: hypoxia ($F_{IO_2} = 0.12$; series I: seven wild-type and nine *Hoxa5*$^{-/-}$ mice) or hypercapnia ($F_{ICO_2} = 0.05$; series II: seven wild-type and eight *Hoxa5*$^{-/-}$ mice). All experiments were performed according to the guidelines of the Canadian Council on Animal Care and approved by the institutional animal care committee.

Measurements of ventilation. Minute ventilation of unrestrained, unanesthetized mice was measured using a whole-body, flow-through plethysmograph (PLY3211, Buxco Electronics, Sharon, CT). The system consisted of a 400 mL Plexiglas experimental chamber equipped with two pneumotachographs with a defined resistance (25). Pressure differences between the experimental and reference chambers were measured with a differential pressure transducer (SenSym, Honeywell, Milpitas, CA) with a fast response time (500 μs). After amplification, the pressure signal was integrated by data analysis software (Buxco Biosystem XA). The system was calibrated by injecting a known volume (0.1 mL) into the chamber with a glass syringe. The barometric pressure and the body weight of each mouse were recorded on the day of the experiment. The chamber temperature and humidity and the rectal temperature of the animals (T_B) were also measured at the beginning and end of each experimental period. These data

Table 1. *Comparison of selected variables between wild-type and Hoxa5*$^{-/-}$ *mice under baseline (air) conditions*

	Wild type (n = 14)	*Hoxa5*$^{-/-}$ (n = 17)
Age (d)	53 ± 2	55 ± 1
Weight (g)	28.4 ± 0.6	29.5 ± 0.6
T_B (°C)	38.8 ± 0.1	38.3 ± 0.2
Breathing frequency (breaths/min)	168 ± 6	214 ± 9*
Tidal volume (mL BTPS)	0.35 ± 0.03	0.38 ± 0.04
Inspiratory flow (mL/s)	2.8 ± 0.2	3.8 ± 0.4*
Minute ventilation (mL BTPS/min)	57 ± 4	79 ± 8*
$\dot{V}_{CO_2}$ (mL BTPS)	1.9 ± 0.2	1.89 ± 0.08
Hb (g/dL)	14.5 ± 0.1 (n = 8)	14.8 ± 0.3 (n = 4)
Hematocrit (%)	45.3 ± 0.6 (n = 8)	46.1 ± 0.7 (n = 4)

Data are presented as means ± 1 SEM. Data were pooled from both series of experiments (hypoxia and hypercapnia) with the exception of the Hb and hematocrit values that were obtained from mice in which lungs were harvested for morphometric analysis.

* Value statistically different from wild-type mice at $p < 0.05$.

were used to express the tidal volume in milliliters BTPS (body temperature, pressure standard). Fresh air (baseline) or gas mixtures were delivered into the experimental chamber at a constant rate with a bias flow regulator (PLY1020; Buxco Electronics). The gas mixture flowing out of the chamber was analyzed with a flow-through capnograph (Novametrix, Wallingford, CT) for subsequent calculation of CO_2 production ($\dot{V}CO_2$) with an open system according to the method and equation described by Mortola and Dotta (26). CO_2 measurements from the outflowing gas mixture also ensured that CO_2 levels within the chamber always remain below 0.5% under baseline conditions. Typical airflow to the chamber ranged between 380 and 400 mL/min.

After the rectal temperature was recorded, the mouse was placed in the plethysmography chamber with room air flowing through. The animal would typically explore the surroundings, groom itself, and then settle down. Baseline measurements were made when the animal was quiet but awake, and breathing room air. Then a gas mixture of either 12% O_2 in N_2 (series I) or 5% CO_2 in air (series II) was delivered to the chamber for 10 min before the chamber was opened for a final body temperature measurement. In each series, animals were only exposed to one respiratory stimulus. All measurements were performed between 1000 and 1500 h.

Sample collection, histology, morphometry, and blood measurements. After ventilation experiments, the wild-type and *Hoxa5*$^{-/-}$ mice were subjected to euthanasia by cervical dislocation and their lungs were recovered and fixed by tracheal instillation with cold 4% paraformaldehyde in PBS until fully inflated under direct observation. Following washes in graded ethanol and embedding in paraffin wax, samples were sectioned (4 μm) and stained according to standard hematoxylin and eosin procedure. Morphometric measurements were performed on four wild-type and six *Hoxa5*$^{-/-}$ mice according to the point counting method (27,28). The overall proportion (% fractional area: % fx area) of respiratory parenchyma and airspace was established for each mouse from 10 randomly selected fields throughout the different lobes taken with a 20× objective. Each field was transferred to a computer screen using the METAMORPH imaging software (Universal Imaging, West Chester, PA). A 180-point lattice grid was superimposed on each image and the number of intersections (points) falling over respiratory parenchyma (alveoli and alveolar ducts) or airspace was counted, excluding points falling over bronchioles, large vessels, smaller arterioles, and venules. The fractional area corresponds to the relative proportion of points intersecting either the respiratory parenchyma or the airspace relatively to the total number of points (parenchyma plus airspace).

Blood was collected from eight wild-type and four *Hoxa5*$^{-/-}$ mice, and the hematocrit and Hb levels were measured using a HMX Beckman Coulter apparatus (Beckman Coulter, Inc., Fullerton, CA).

For histologic analyses of isolated tracheas, specimens were dissected from adult animals (two wild-type and two *Hoxa5*$^{-/-}$ mice) subjected to euthanasia by CO_2 inhalation. The tracheas were fixed and treated as above, and 4 μm sections were stained according to standard hematoxylin and eosin procedure. Tracheal lumen diameter was measured using a micrometer.

Statistical analysis. A mixed model ANOVA was used with field as random effect and genotype as fixed effect in analyses of % Fx area. Measurements of ventilatory variables were obtained by averaging 3–4 min of stable recording either under baseline (air) or at the end of hypoxic or hypercapnic stimulus. Breathing pattern comparisons between wild-type and *Hoxa5*$^{-/-}$ mice under baseline conditions (normoxia, normocapnia) was performed by pooling ventilatory data obtained from both series of experiments. These results were analyzed statistically using a one-way ANOVA (genotype effect). Between-group comparisons of the ventilatory measurements during hypoxia (series I) or hypercapnia (series II) were performed using a two-way ANOVA for repeated measures (stimulus × genotype). In both series, mean frequency data were also analyzed for each minute of the hypoxic or hypercapnic stimulus to compare the temporal dynamics of the response (Δ frequency) between genotypes with a two way ANOVA for repeated measures (time × genotype). Responsiveness to ventilatory stimuli was assessed by expressing data as the percentage change relative to baseline measurements; these data were statistically analyzed using a one-way ANOVA. These analyses were followed by a posthoc Fisher's protected least squares difference test when appropriate ($p < 0.05$). Statistical analyses were done with StatView version 5.0 (SAS Institute, Cary, NC).

A Mann-Whitney test for nonparametric data was used to compare the mean of hematocrit and Hb concentrations.

RESULTS

Lung and trachea morphology in* Hoxa5$^{-/-}$ *mice. We had previously observed in *Hoxa5*$^{-/-}$ surviving adult mice gross anomalies at the lung periphery, suggesting septation defects (2). The lungs were clearly diseased, with regions devoid of pulmonary alveoli or displaying large tubular structures. Tissue sections of lungs from adult mice showed a picture reminiscent of lung emphysema with enlargement of alveolar airspaces, short or inexistent septa, and oversimplified alveolar architecture (Fig. 1*A*). Morphometric analyses of lungs from *Hoxa5*$^{-/-}$ mice were consistent with the histologic data and the relative proportion of airspace was increased by 52% ($p = 0.00001$) in mutants compared with wild-type specimens. Additionally, the percentage of fractional area of respiratory parenchyma was diminished significantly in *Hoxa5*$^{-/-}$ mice (49% parenchyma/51% airspace *versus* 22% parenchyma/78% airspace for wild-type and *Hoxa5*$^{-/-}$ mice, respectively; Fig. 1*B*).

We had reported a reduction of the diameter of the tracheal lumen of *Hoxa5*$^{-/-}$ newborn pups that is likely the cause of the rapid perinatal death in the most severely affected specimens (20). To determine the status of the trachea in adult mice, we compared tracheal lumen diameter between genotypes by histologic examinations of transverse sections. Although the mutant tracheal epithelium retained its pseudostratified characteristic, the cellular density seemed increased compared with the wild-type one. In addition, the lamina propria was hypertrophied (Fig. 2). The lumen of the trachea was also narrower (0.92 ± 0.07 mm) than that of control animals from the same

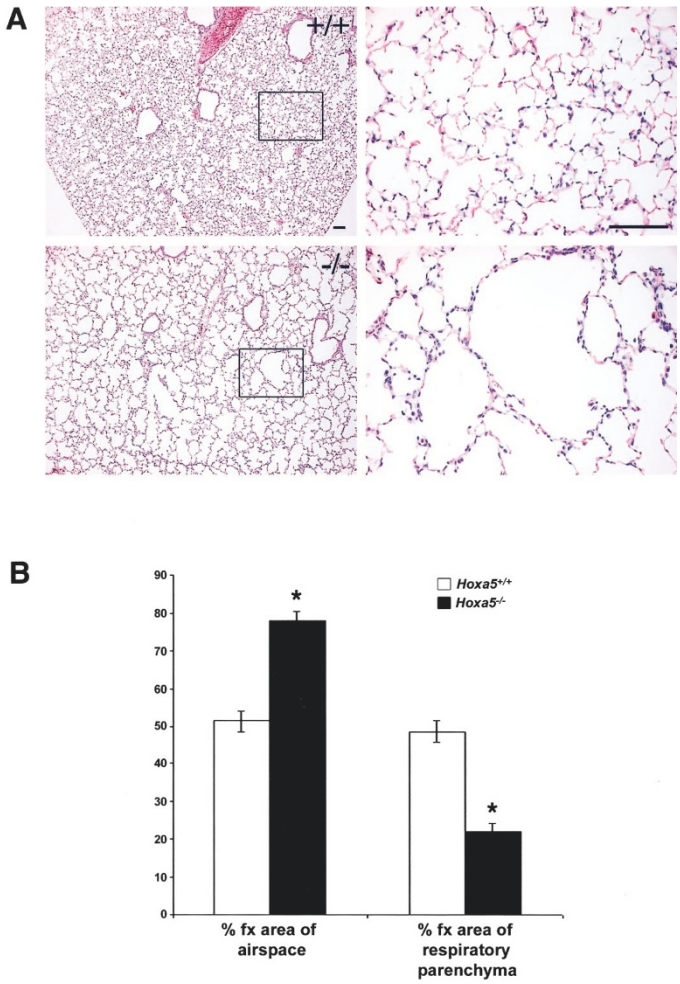

Figure 1. Comparative histologic and morphometric analyses of lungs from wild-type (+/+) and *Hoxa5* homozygous mutant (−/−) mice subjected to euthanasia at 60 d of age. (*A*) Sections of lungs were stained with hematoxylin and eosin revealing a severe emphysematous-like phenotype in *Hoxa5*$^{-/-}$ lungs characterized by an enlargement of the airspaces and an overall decrease in septa number. The *Hoxa5*$^{-/-}$ specimen shown is representative of all the samples analyzed. (*B*) Comparison of the % fractional area (% fx area) of airspace and respiratory parenchyma between controls and mutant lungs revealed that the % fx area of airspace is significantly increased by 52% in *Hoxa5*$^{-/-}$ lungs. *Mean value statistically different from corresponding wild-type value at $p = 0.00001$. Scale bar: 100 μm.

age (1.34 ± 0.22 mm), but the phenotype was less dramatic than that reported in newborn mutant pups (20). These observations were consistent with the fact that the surviving animals were the least affected mutants.

At the time of experimentation (around 8 wk of age), the body weight of the animals was not significantly different between wild-type and *Hoxa5*$^{-/-}$ mice (Table 1), in accordance with our previous observations (23). In addition, no significant difference was observed in lung weight-to-body weight ratio between both genotypes ($p = 0.95$; data not shown), indicating that despite a decreased lung surface area, the *Hoxa5*$^{-/-}$ mice were able to develop as well as their wild-type littermates.

Resting breathing pattern and blood respiratory variables in wild-type and* Hoxa5 *mutant mice. To determine whether the abnormal lung morphology associated with the *Hoxa5* mutation affects breathing pattern, we first measured the respiratory cycle of both mouse lines in resting conditions. While breathing air, minute ventilation of *Hoxa5*$^{-/-}$ mice was 39% greater than that of wild-type animals ($p = 0.03$; Table 1). This enhancement of basal ventilatory activity was due exclusively to higher breathing frequency ($p = 0.0003$; Table 1), as tidal volume was not significantly different between both genotypes ($p = 0.63$; Fig. 3). Figure 3 shows representative plethysmographic recordings obtained for both genotypes, and compares spirograms for a single respiratory cycle between wild-type and *Hoxa5*$^{-/-}$ mice. These data show that the higher breathing frequency of *Hoxa5* mutants was due to a shortening of the respiratory cycle; that is, both inspiratory (T_I) and expiratory (T_E) times of *Hoxa5*$^{-/-}$ mice were shorter than those of wild-type animals ($p = 0.0002$ and $p = 0.003$ for T_I and T_E, respectively). Thus, to achieve a tidal volume comparable to that of wild-type mice, *Hoxa5* mutants had to generate a higher inspiratory flow ($p = 0.04$; Table 1; Fig. 3).

Analysis of blood hematocrit and Hb concentration revealed no significant differences between groups, thereby suggesting that O_2 carrying capacity was similar for control and *Hoxa5*$^{-/-}$ mice ($p = 0.50$ and $p = 0.44$ for hematocrit and Hb concentrations, respectively; Table 1). In addition, mean CO_2 production was not different between the two genotypes ($p = 0.80$; Table 1).

Series I: Ventilatory response to hypoxia. Genetic factors have been associated with the wide variability in the magnitude of ventilatory responses to hypoxia and hypercapnia (29). Therefore, we tested whether the *Hoxa5* gene was functionally involved in the respiratory control system. In the minutes that followed initiation of hypoxia, mice showed a progressive increase in breathing frequency (time effect: $p < 0.0001$; Fig. 4). Although breathing frequency change did not differ between both mouse lines ($p = 0.95$), the between-factor interaction was significant, thus indicating that the dynamic of the response was genotype-dependent (genotype × time: $p = 0.0015$; Fig. 4). Unlike wild-type mice, *Hoxa5*$^{-/-}$ animals could not sustain their initial frequency increase throughout the entire hypoxic episode.

Ventilatory measurements obtained at the end of the hypoxic episode showed that minute ventilation was higher than the baseline (Fig. 5*A*; $p < 0.0001$). Although minute ventilation seemed higher in *Hoxa5*$^{-/-}$ than in wild-type mice, the difference was not statistically significant (Fig. 5*A*; $p = 0.07$). Breathing frequency also increased for both genotypes during hypoxia to reach a similar value (Fig. 5*B*; $p < 0.0001$). The increase in breathing frequency for both wild-type and *Hoxa5*$^{-/-}$ mice was due to a shortening of T_I AND T_E ($p = 0.003$ and $p = 0.0004$, respectively). Although there was no significant difference between both genotypes ($p = 0.13$), the between-factor interaction shows that the breathing frequency response to hypoxia was genotype-dependent (hypoxia × genotype: $p = 0.05$). Tidal volume also contributed to the minute ventilation increase during hypoxia (Fig. 5*C*; $p = 0.047$); however, this increase was significant only in *Hoxa5*$^{-/-}$ mice. Despite suggestive trends, ANOVA indicates that the tidal volume was not significantly different between wild-type and mutant mice (Fig. 5*C*; $p = 0.12$).

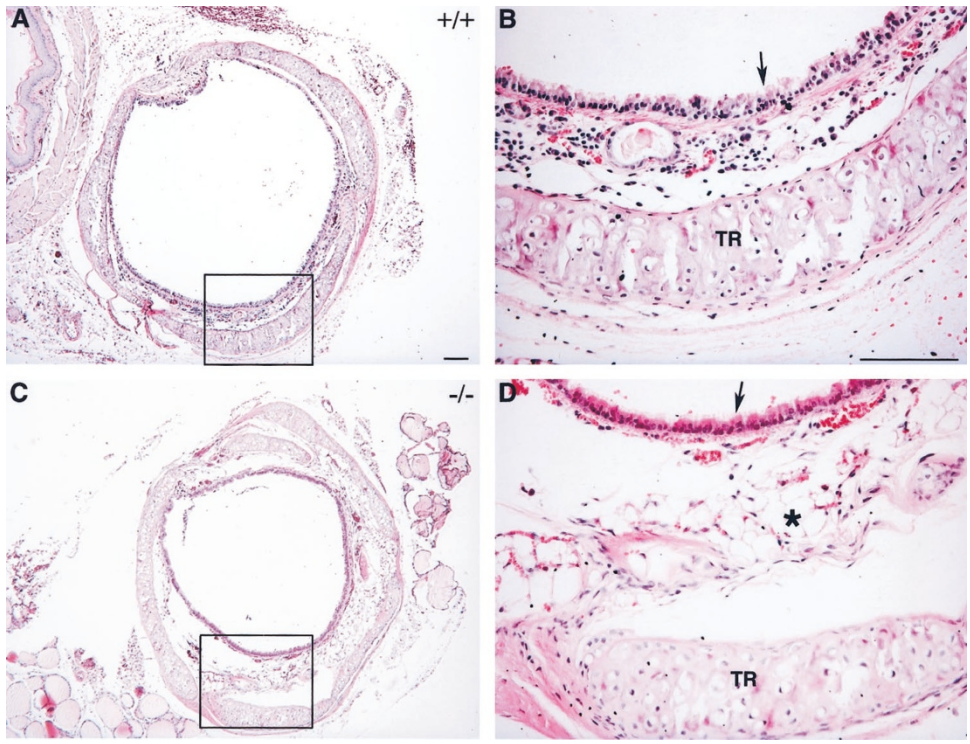

Figure 2. Comparative histologic analysis of the trachea from wild-type (+/+) and *Hoxa5* homozygous mutant (−/−) mice subjected to euthanasia at 7–8 mo of age. Transverse sections were stained with hematoxylin and eosin revealing a reduction of the lumen diameter, a disorganization of the epithelia (*arrows*) and a thickening of the submucosa (*) in *Hoxa5* mutants (*C, D*) when compared with wild-type specimens (*A, B*). *TR,* tracheal ring. Scale bar: 100 μm.

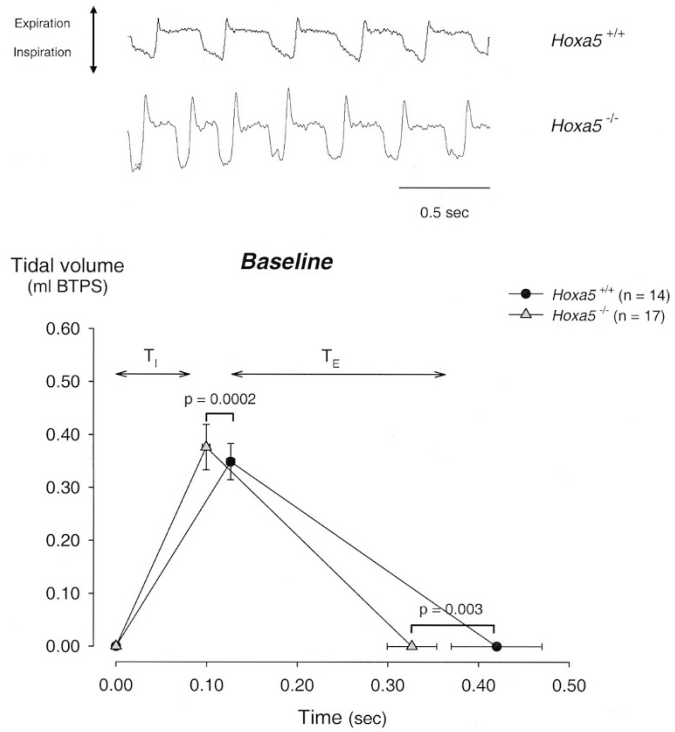

Figure 3. Plethysmographic recordings comparing the breathing pattern of wild-type and *Hoxa5* mutant mice breathing room air (*top panel*). The bottom panel shows a spirogram comparing an average respiratory cycle between wild-type (*Hoxa5*$^{+/+}$; *black circles*, $n = 14$) and *Hoxa5* mutant mice (*Hoxa5*$^{-/-}$; *gray triangles*, $n = 17$) under baseline conditions (room air). These data were obtained by pooling baseline values measured in both experimental series (hypoxia and hypercapnia). Data are expressed as means ± 1 SEM.

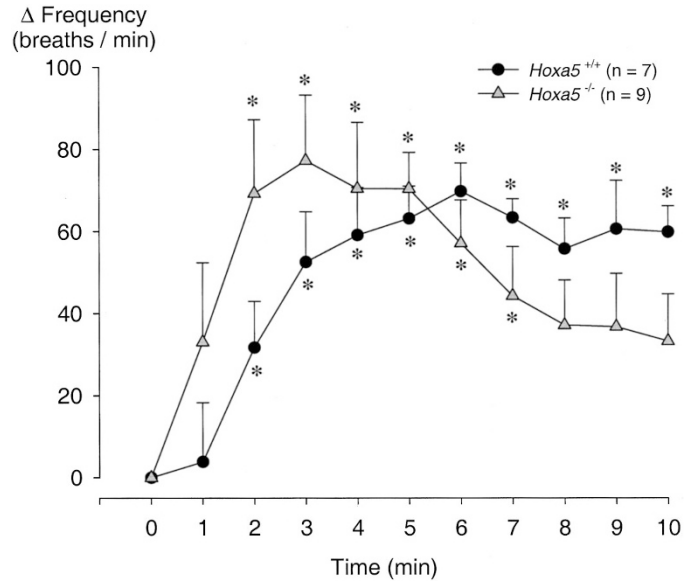

Figure 4. Temporal dynamics of the breathing frequency response (expressed as change from baseline) to hypoxia ($F_{IO_2} = 0.12$) in wild-type (*Hoxa5*$^{+/+}$; *black circles*, $n = 7$) and *Hoxa5* mutant mice (*Hoxa5*$^{-/-}$; *gray triangles*, $n = 9$). *Mean value significantly different from baseline at $p < 0.05$.

To further characterize the functional differences between wild-type and *Hoxa5*$^{-/-}$ mice during exposure to a hypoxic challenge, selected ventilatory variables were normalized and expressed as a percentage change from baseline values (Fig. 6). This additional analysis confirmed that the minute ventilation response to hypoxia did not differ between genotypes ($p = 0.75$), even though the frequency response of mutants was less

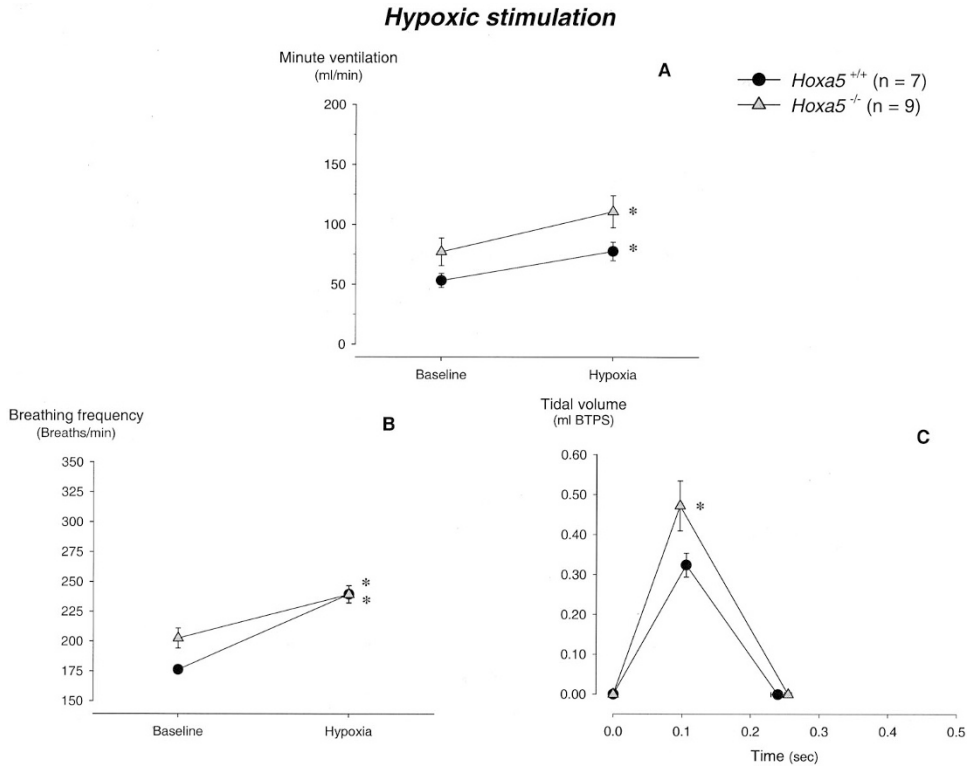

Figure 5. Hypoxic ventilatory response in wild-type (*Hoxa5*$^{+/+}$; *black circles*, $n = 7$) and *Hoxa5* mutant mice (*Hoxa5*$^{-/-}$; *gray triangles*, $n = 9$). Minute ventilation (*A*) and breathing frequency (*B*) were measured while the animal was under baseline condition (air) and after 10 min of exposure to moderate hypoxia ($Fio_2 = 0.12$). The spirogram shown in *panel C* compares an average breathing cycle for both genotypes at the end of the hypoxic challenge. Tidal volume increase was observed in mutant mice only; mean inspiratory flow of mutant mice was significantly greater than that of wild-type. Values are expressed as means ± SEM. *Mean value statistically different from baseline at $p < 0.05$.

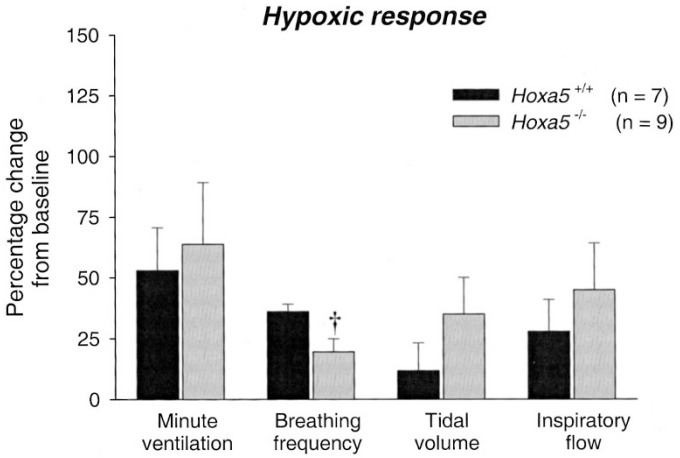

Figure 6. Normalized ventilatory response to hypoxia ($Fio_2 = 0.12$; series I) in wild-type (*Hoxa5*$^{+/+}$; *black bars*, $n = 7$) and *Hoxa5* mutant mice (*Hoxa5*$^{-/-}$; *gray bars*, $n = 9$). Percentage changes from normoxic baseline values in minute ventilation, breathing frequency, tidal volume, and inspiratory flow were obtained 10 min after the hypoxic stimulus. Data expressed as means ± 1 SEM. †Mean statistically different from corresponding wild-type value at $p < 0.05$.

than that of wild-type mice ($p = 0.03$). The latter result confirms the previous analysis on absolute frequency data showing that the frequency response was genotype-dependent (Fig. 5*B*). Expressing tidal volume or inspiratory flow as a percentage change from baseline revealed no difference between wild-type and mutant animals ($p = 0.26$ and $p = 0.5$, respectively; Fig. 6).

Series II: Ventilatory response to hypercapnia. Upon initiation of the hypercapnic stimulus, mice showed a rapid increase in breathing frequency (time effect: $p < 0.0001$; Fig. 7). The breathing frequency change did not differ between both

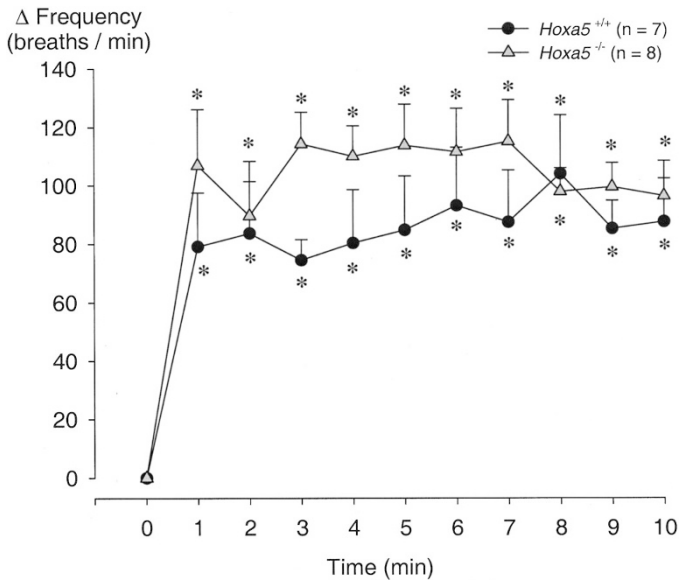

Figure 7. Temporal dynamics of the breathing frequency response (expressed as change from baseline) to hypercapnia ($Fico_2 = 0.05$) in wild-type (*Hoxa5*$^{+/+}$; *black circles*, $n = 7$) and *Hoxa5* mutant mice (*Hoxa5*$^{-/-}$; *gray triangles*, $n = 8$). *Mean value significantly different from baseline at $p < 0.05$.

mouse lines ($p = 0.19$), and unlike the hypoxic response, the statistical analysis did not indicate that the dynamic of the frequency response was genotype-dependent (genotype × time: $p = 0.69$; Fig. 7). Both groups of mice were able to sustain their breathing frequency increase throughout the entire hypercapnic episode.

Exposing mice to moderate hypercapnia increased minute ventilation equally in both experimental groups (hypercapnia effect: $p = 0.0006$; genotype effect: $p = 0.35$; Fig. 8*A*). This augmentation in ventilatory activity was due to an important increase in breathing frequency and a less dramatic one in tidal volume ($p < 0.0001$ and $p = 0.01$, respectively; Fig. 8, *B* and *C*). Breathing frequency was higher in *Hoxa5*$^{-/-}$ mice than in controls ($p = 0.01$), but the responsiveness to the stimulus was similar for both groups (hypercapnia × genotype: $p = 0.99$). To achieve this breathing frequency during hypercapnia, T_I and T_E of *Hoxa5*$^{-/-}$ mice were shorter than those of wild-type animals (Fig. 8*C*). Moreover, during hypercapnia, T_E shortening was greater in *Hoxa5*$^{-/-}$ mice (hypercapnia × genotype: $p = 0.002$). Inspiratory flow increased marginally during hypercapnia ($p = 0.072$); however, there was no significant difference between genotypes ($p = 0.2$; Fig. 8*C*).

Expressing ventilatory data as a percentage change from baseline values allowed further comparison of the hypercapnic ventilatory response between wild-type and mutant mice and confirmed that the minute ventilation response to hypercapnia did not differ between them ($p = 0.84$; Fig. 9). Although the frequency response of *Hoxa5*$^{-/-}$ mice appeared to be less than that of wild-type mice ($p = 0.07$; Fig. 9), this result should be interpreted cautiously given the large difference in resting breathing frequency between the two groups (Fig. 8*B*). Expressing tidal volume or inspiratory flow as a percentage change from baseline revealed no differences between genotypes ($p = 0.63$ and $p = 0.71$, respectively; Fig. 9).

DISCUSSION

To our knowledge, the present study represents one of the first attempts at examining the consequences of the loss of *Hox* gene function on adult respiratory physiology using the *Hoxa5* mutant mouse line as a model. In absence of *Hoxa5* function, adult lungs harbor emphysema-like characteristics and the tracheal lumen is narrowed. In addition, the respiratory control system of *Hoxa5* mutant mice differs from that of wild-type animals, thereby providing yet another manifestation of the adaptability of the respiratory control system. Although mainly descriptive in nature, the between-group differences observed nonetheless provide valuable information concerning the putative strategies allowing survival of *Hoxa5*$^{-/-}$ mice facing a reduction in trachea lumen diameter and a significant deficit in gas exchange capacity.

Baseline breathing pattern in* Hoxa5$^{-/-}$ *mice. *Hoxa5*$^{-/-}$ mice compensate for their reduced lung alveolar surface available for gas exchange by increasing minute ventilation. Based on indirect assessment of metabolism (*via* $\dot{V}_{CO_2}$ measurements and body weight), our data suggest that the higher resting

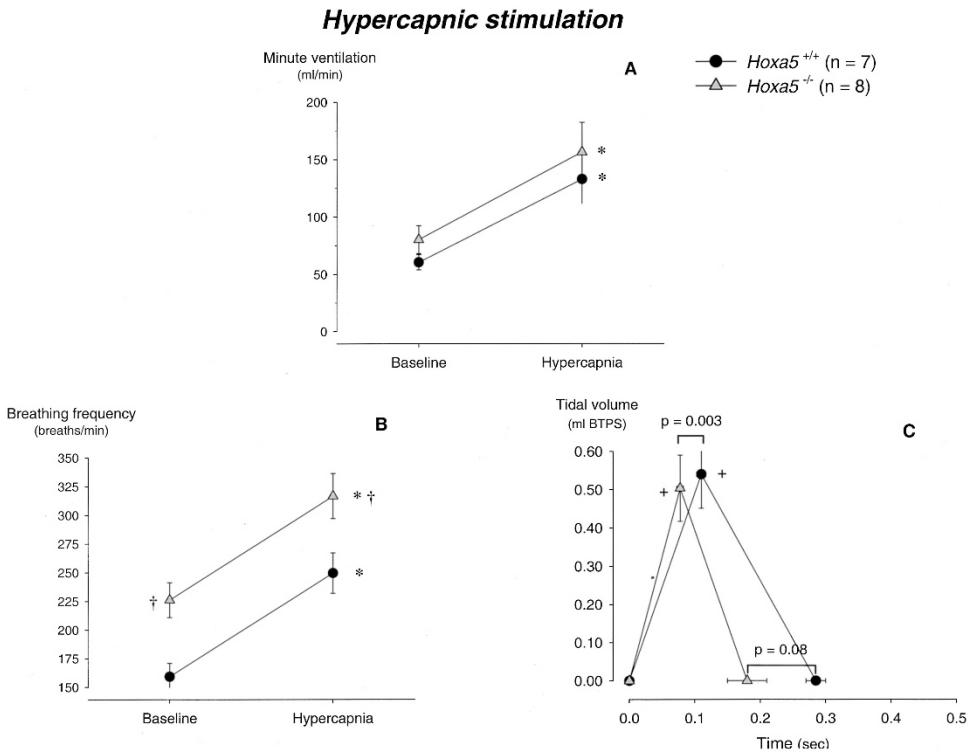

Figure 8. Hypercapnic ventilatory response in wild-type (*Hoxa5*$^{+/+}$; *black circles*, $n = 7$) and *Hoxa5* mutant mice (*Hoxa5*$^{-/-}$; *gray triangles*, $n = 8$). Minute ventilation (*A*) and breathing frequency (*B*) were measured while the animal was under baseline condition (air) and after 10 min of exposure to moderate hypercapnia ($Fi_{CO_2} = 0.05$). The spirogram shown in *panel C* compares an average breathing cycle for both genotypes at the end of the hypercapnic challenge. Values are expressed as means ± SEM *Mean value significantly different from baseline at $p < 0.05$. $^{+}$Mean value statistically different from baseline at $p < 0.1$. †Mean statistically different from corresponding wild-type value at $p < 0.05$.

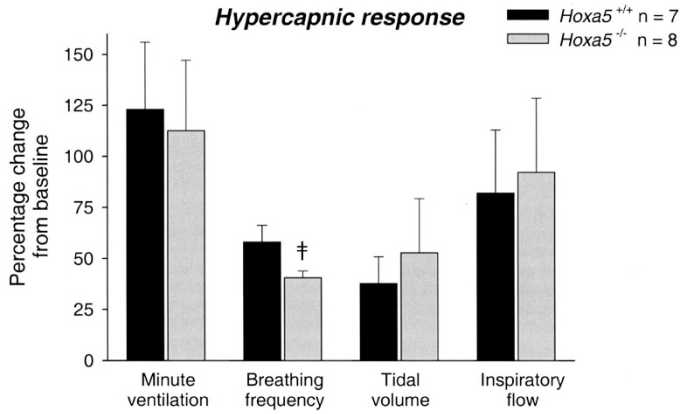

Figure 9. Normalized ventilatory response to hypercapnia (F_{ICO_2} = 0.05; series II) in wild-type (*Hoxa5*$^{+/+}$; *black bars*, n = 7) and *Hoxa5* mutant mice (*Hoxa5*$^{-/-}$; *gray bars*, n = 8). Percentage changes from normoxic baseline values in minute ventilation, breathing frequency, tidal volume, and inspiratory flow were obtained 10 min after the hypercapnic stimulus. Data expressed as means ± 1 SEM. ‡Mean statistically different from corresponding wild-type value at $p < 0.1$.

minute ventilation of *Hoxa5*$^{-/-}$ mice reflects an increased convective requirement that can be attributed mainly to a reduction in gas exchange efficiency rather than to a metabolic need. Given that oxygen carrying capacity was similar between both groups and that mammals tend to adjust their breathing frequency and tidal volume to minimize the mechanical work of ventilation, our data suggest that, in *Hoxa5*$^{-/-}$ mice, increasing breathing frequency is an efficient adaptive mean to meet gas exchange requirements, thus preventing hypoxemia (30).

Accordingly, the increased inspiratory flow of *Hoxa5*$^{-/-}$ mice reflects the need to generate a greater inspiratory effort to achieve the same tidal volume as wild-type mice over a shorter period of time (reduced T_I, increased breathing frequency) while facing a greater upper airway resistance, most likely caused by the decreased trachea diameter.

Both genotypes had similar lung to body weight ratio at adult ages despite some growth retardation shortly after birth (23; M. LeBlanc and L. Jeannotte, unpublished observations). Although *Hoxa5* mutant lung presented an emphysema-like architecture, the breathing pattern of *Hoxa5* mutant mice varies from that of subjects suffering from obstructive diseases, inasmuch as, in the latter case, the tidal volume is greater, the expiratory flow is diminished, and an important residual volume remains trapped in the lung (31). Whereas emphysema has been defined as abnormal permanent enlargement of airspaces accompanied by destruction of their walls (32), the *Hoxa5* mutant lung phenotype appears to result from defective alveogenesis, indicating a different etiology (M. LeBlanc, I. Mandeville, and L. Jeannotte, unpublished observations).

The disruption of lung development observed in *Hoxa5*$^{-/-}$ mice is also comparable to the impaired alveolarization following neonatal hyperoxia (30,33), but the effects on breathing pattern differ substantially. For instance, adult mice subjected to neonatal hyperoxia show a greater tidal volume and a lower breathing frequency than control mice, with no net difference in resting minute ventilation between groups. These differences between the two studies might be explained by the reduced trachea diameter observed in *Hoxa5*$^{-/-}$ mice that likely increases airways resistance in these animals.

Hypoxic ventilatory response. The ventilatory response to hypoxia has several time domains involving different physiologic mechanisms (34). The immediate augmentation of ventilatory activity at the onset of hypoxia, termed the acute response, is normally attributed to the increase in chemoreceptor afferent input at the level of the CNS (34,35). The initial breathing frequency increase of *Hoxa5*$^{-/-}$ mice is greater than that of control animals, suggesting that chemoafferent input may be more important in the mutant group. Recent analysis of the mutation of the paired-like homeobox gene *Phox2b* has shown that perturbation of the carotid body development alters the ventilatory response of *Phox2b* mutants to both hypoxia and hypercapnia (36). Although such experiments are beyond the scope of the present study, electrophysiological assessment of carotid body function could determine whether sensing of hypoxic and hypercapnic stimuli is altered in *Hoxa5* mutants. A greater chemosensitivity may be part of a series of physiologic strategies aimed at protecting these mice from fluctuations of arterial blood gases given the reduced alveolar surface available for gas exchange. On the other hand, the ventilatory response of *Hoxa5*$^{-/-}$ mice to hypercapnia was similar to that observed in wild-type animals suggesting that the carotid body may not be involved or, if so, the alteration of the chemoreflex is stimulus specific. It was recently shown that *Hoxa3*$^{-/-}$ mice lack carotid body due to the defective development of the third arch artery, which results in the malformation of the carotid artery system (37). However, because *Hoxa3*$^{-/-}$ pups die at birth or shortly thereafter, no data are available on the functional consequences of the *Hoxa3* mutation on respiration and chemoreflexes (18). Based on previous work on animals and humans with denervated or resected carotid bodies, a negligible response to hypoxia should be expected in *Hoxa3*$^{-/-}$ animals (38). In contrast to the *Hoxa3* gene, *Hoxa5* is not expressed in the third branchial arch from which the carotid body derives. However, *Hoxa5* transcripts are detected in the mesenchyme adjoining various organs from the cervical region raising the possibility that *Hoxa5* may indirectly act on carotid body development and function (20,23).

In wild-type mice, a steady breathing frequency characterizes the second phase of the hypoxic ventilatory response. Unlike control mice, *Hoxa5*$^{-/-}$ mice showed short-term depression of breathing frequency during the last 5 min of hypoxic stimulation, indicating that these animals are unable to sustain the initial frequency increase throughout the entire hypoxic period. Expressing ventilatory data obtained at the end of the hypoxic protocol as a percentage change from baseline confirmed that the frequency component of the response was less in the *Hoxa5*$^{-/-}$ group, although the hypoxic ventilatory response was similar in both genotypes. These data indicate that the acute frequency response is a transient overshoot that may reflect an increased sensitivity of *Hoxa5*$^{-/-}$ mice to hypoxia.

The absence of a tidal volume increase during hypoxia in wild-type mice is consistent with previous reports (30,39,40). The significant tidal volume increase observed in *Hoxa5*$^{-/-}$ mice does not reflect an inability to further increase breathing frequency since mutant mice exposed to hypercapnia breathe at

a much faster rate. It is thus possible that while facing a hypoxic challenge, mutant mice increase their tidal volume to improve gas exchange effectiveness at a minimal cost by reducing the V_D/V_T ratio.

Hypercapnic ventilatory response. Exposing mice to a hypercapnic challenge revealed no functional difference between genotypes besides the higher breathing frequency (and shorter respiratory cycle) discussed previously. The marginal reduction in the breathing frequency response to hypercapnic challenge observed in mutant mice is unclear, but may reflect a ceiling effect given that the mean frequency measured during hypercapnia in mutant mice was the highest observed for the entire study.

Hox *genes and respiratory phenotype.* Several experimental evidences demonstrate the importance of *Hox* genes as genetic determinants of the respiratory control system. For instance, newborn *Hoxa1* mutant mice in which hindbrain segmentation is disrupted are characterized by a variable respiratory frequency that will ultimately lead to premature death (17). Furthermore, transcriptional regulators for *Hox* gene expression, such as Krox20 and kreisler, were shown to be implicated in the control of breathing (41–43). Both *Krox20* and *kreisler* genes are involved in hindbrain segmentation and their loss of function results in distinct respiratory phenotypes associated with defects of central components of the respiratory control system (44,45). Unlike *Hox* mutants in which abnormal hindbrain segmentation causes respiratory defects, the respiratory activity of *Hoxa5*$^{-/-}$ mice is rhythmic and regular. Moreover, the response to ventilatory stimuli can be considered adequate, despite some variations when compared with wild-type specimens. The cause of death of *Hoxa5* mutants is not due to an abnormal breathing pattern but to anatomical defects that profoundly affect the respiratory tract *per se* and reflect the expression pattern of *Hoxa5* along the respiratory system. These deficiencies cause respiration obstruction in the more severe cases (20). As observed in several organ systems, the respiratory phenotypes observed in *Hox* mutants further endorse the collinear relationship existing between the position of each *Hox* gene within the *Hox* cluster and the defects associated with each mutation (2).

CONCLUSION

Hoxa5$^{-/-}$ mice compensate for their increased airway resistance and reduced alveolar surface area available for gas exchange by a higher breathing frequency and overall minute ventilation. The high inspiratory flows produced by *Hoxa5*$^{-/-}$ mice suggest that, in these animals, the reduced trachea lumen diameter is a limiting factor that may also contribute to the adaptability reported in this study. We hypothesize that these anatomical limitations make it difficult to maintain blood gas homeostasis during sleep, and that the ensuing intermittent bouts of hypoxemia contribute to the enhanced responsiveness to acute hypoxia in *Hoxa5*$^{-/-}$ animals (46), which, in turn, help maintain respiratory homeostasis.

Acknowledgments. The authors thank Drs. Josée Aubin and Jean Charron for insightful comments on the manuscript and Ms. Lucie Ouellette from the Department of Hematology from L'Hôtel-Dieu de Québec for technical help with the hematocrit and Hb measurements.

REFERENCES

1. Krumlauf R 1994 *Hox* genes in vertebrate development. Cell 78:191–201
2. Aubin J, Jeannotte L 2001 Implication des gènes *Hox* dans les processus d'organogénèse chez les mammifères. Médecine/Sciences 17:54–62
3. Pasqualetti M, Rijli FM 2001 Homeobox gene mutations and brain-stem developmental disorders: learning from knockout mice. Curr Opin Neurol 14:177–184
4. Trainor PA, Krumlauf R 2001 *Hox* genes, neural crest cells and branchial arch patterning. Curr Opin Cell Biol 13:698–705
5. Carpenter EM 2002 *Hox* genes and spinal cord development. Dev Neurosci 24:24–34
6. Goodman FR 2003 Congenital abnormalities of body patterning: embryology revisited. Lancet 362:651–662
7. Wellik DM, Capecchi MR 2003 *Hox10* and *Hox11* genes are required to globally pattern the mammalian skeleton. Science 301:363–367
8. Godwin AR, Capecchi MR 1998 Hoxc13 mutant mice lack external hair. Genes Dev 12:11–20
9. Chen H, Sukumar S 2003 Role of homeobox genes in normal mammary gland development and breast tumorigenesis. J Mammary Gland Biol Neoplasia 8:157–173
10. Economides KD, Capecchi MR 2003 Hoxb13 is required for normal differentiation and secretory function of the ventral prostate. Development 130:061–2069
11. Bogue CW, Gross I, Vasavada H, Dynia DW, Wilson CM, Jacobs HC 1994 Identification of *Hox* genes in newborn lung and effects of gestational age and retinoic acid on their expression. Am J Physiol 266:L448–L454
12. Cardoso WV 1995 Transcription factors and pattern formation in the developing lung. Am J Physiol 269:L429–L442
13. Kappen C 1996 *Hox* genes in the lung. Am J Respir Cell Mol Biol 15:156–162
14. Mollard R, Dziadek M 1997 Homeobox genes from clusters A and B demonstrate characteristics of temporal colinearity and differential restrictions in spatial expression domains in the branching mouse lung. Int J Dev Biol 41:655–666
15. Lufkin T, Dierich A, LeMeur M, Mark M, Chambon P 1991 Disruption of the *Hox-1.6* homeobox gene results in defects in a region corresponding to its rostral domain of expression. Cell 66:1105–1119
16. Chisaka O, Musci TS, Capecchi MR 1992 Developmental defects of the ear, cranial nerves and hindbrain resulting from targeted disruption of the mouse homeobox gene. Hox-1.6. Nature 355:516–520
17. del Toro ED, Borday V, Davenne M, Neun R, Rijli FM, Champagnat J 2001 Generation of a novel functional neuronal circuit in *Hoxa1* mutant mice. J Neurosci 21:5637–5642
18. Chisaka O, Capecchi MR 1991 Regionally restricted developmental defects resulting from targeted disruption of the mouse homeobox gene. Hox-1.5. Nature 350:473–479
19. Manley NR, Capecchi MR 1995 The role of *Hoxa-3* in mouse thymus and thyroid development. Development 121:1989–2003
20. Aubin J, Lemieux M, Tremblay M, Bérard J, Jeannotte L 1997 Early postnatal lethality in *Hoxa-5* mutant mice is attributable to respiratory tract defects. Dev Biol 192:432–445
21. Jeannotte L, Lemieux M, Charron J, Poirier F, Robertson EJ 1993 Specification of axial identity in the mouse: role of the *Hoxa-5* (*Hox1.3*) gene. Genes Dev 7:2085–2096
22. Golpon HA, Geraci MW, Moore MD, Miller HL, Miller GJ, Tuder RM, Voelkel NF 2001 HOX genes in human lung—altered expression in primary pulmonary hypertension and emphysema. Am J Pathol 158:955–966
23. Meunier D, Aubin J, Jeannotte L 2003 Perturbed thyroid morphology and transient hypothyroidism symptoms in *Hoxa5* mutant mice. Dev Dyn 227:367–378
24. Aubin J, Lemieux M, Tremblay M, Behringer R, Jeannotte L 1998 Transcriptional interferences at the *Hoxa4*/*Hoxa5* locus: Importance of correct *Hoxa5* expression for the proper specification of the axial skeleton. Dev Dyn 212:141–156
25. Kinkead R, Dupenloup L, Valois N, Gulemetova R 2001 Stress-induced attenuation of the hypercapnic ventilatory response in awake rats. J Appl Physiol 90:1729–1735
26. Mortola JP, Dotta A 1992 Effects of hypoxia and ambient temperature on gaseous metabolism of newborn rats. Am J Physiol 263:R267–R272
27. Bolender RP, Hyde DM, Dehoff RT 1993 Lung morphometry: a new generation of tools and experiments for organ, tissue, cell, and molecular biology. Am J Physiol 265:L521–L548
28. Wert SE, Yoshida M, LeVine AM, Ikegami M, Jones T, Ross GF, Fisher JH, Korfhagen TR, Whitsett JA 2000 Increased metalloproteinase activity, oxidant production, and emphysema in surfactant protein D gene-inactivated mice. Proc Natl Acad Sci U S A 97:5972–5977
29. Gaultier C, Guilleminault C 2001 Genetics, control of breathing, and sleep-disordered breathing: a review. Sleep Med 2:281–295
30. Dauger S, Ferkdadji L, Saumon G, Vardon G, Peuchmaur M, Gaultier C, Gallego J 2003 Neonatal exposure to 65% oxygen durably impairs lung architecture and breathing pattern in adult mice. Chest 123:530–538
31. Hlastala MP, Berger AJ 1996 Physiology of Respiration. Oxford University Press, New York

32. Hogg JC 2001 Chronic obstructive pulmonary disease: an overview of pathology and pathogenesis. Novartis Foundation Symp 234:4–26
33. Massaro D, Massaro GD 2002 Invited review: pulmonary alveoli: formation, the "call for oxygen", and other regulators. Am J Physiol Lung Cell Mol Physiol 282:L345–L358
34. Powell FL, Milsom WK, Mitchell GS 1998 Time domains of the hypoxic ventilatory response. Respir Physiol 112:123–134
35. McCrimmon DR, Mitchell GS, Dekin M 1995 Glutamate, GABA, and serotonin in ventilatory control. In: Dempsey JA, Pack AI (eds) Lung Biology in Health and Disease. Marcel Dekker, New York, pp 151–218
36. Dauger S, Pattyn A, Lofaso F, Gaultier C, Goridis C, Galego J, Brunet JF 2003 Phox2b controls the development of peripheral chemoreceptors and afferent visceral pathways. Development 130:6635–6642
37. Kameda Y, Nishimaki T, Takeichi M, Chisaka O 2002 Homeobox gene *Hoxa3* is essential for the formation of the carotid body in the mouse embryos. Dev Biol 247:197–209
38. Honda Y 1992 Respiratory and circulatory activities in carotid-body-resected humans. J Appl Physiol 73:1–8
39. Huey KA, Low MJ, Kelly MA, Juarez R, Szewczak JM, Powell FL 2000 Ventilatory responses to acute and chronic hypoxia in mice: effects of dopamine d(2) receptors. J Appl Physiol 89:1142–1150
40. Renolleau S, Dauger S, Vardon G, Levacher B, Simonneau M, Yanagisawa M, Gaultier C, Gallego J 2001 Impaired ventilatory responses to hypoxia in mice deficient in endothelin-converting-enzyme-1. Pediatr Res 49:705–712
41. Sham MH, Vesque C, Nonchev S, Marshall H, Frain M, Gupta RD, Whiting J, Wilkinson D, Charnay P, Krumlauf R 1993 The zinc finger gene *Krox20* regulates *HoxB2* (*Hox2.8*) during hindbrain segmentation. Cell 72:183–196
42. Manzanares M, Cordes S, Kwan CT, Sham MH, Barsh GS, Krumlauf R 1997 Segmental regulation of *Hoxb-3* by *kreisler.* Nature 387:91–195
43. Manzanares M, Nardelli J, Gilardi-Hebenstreit P, Marshall H, Giudicelli F, Martinez-Pastor MT, Krumlauf R, Charnay P 2002 Krox20 and kreisler co-operate in the transcriptional control of segmental expression of *Hoxb3* in the developing hindbrain. EMBO J 21:365–376
44. Jacquin TD, Borday V, Schneider-Maunoury S, Topilko P, Ghilini G, Kato F, Charnay P, Champagnat J 1996 Reorganization of pontine rhythmogenic neuronal networks in *Krox-20* knockout mice. Neuron 17:747–758
45. Chatonnet F, del Toro ED, Voiculescu O, Charnay P, Champagnat J 2002 Different respiratory control systems are affected in homozygous and heterozygous kreisler mutant mice. Eur J Neurosci 15:684–692
46. Mitchell GS, Johnson SM 2003 Neuroplasticity in respiratory motor control. J Appl Physiol 94:358–374